Origins of High Sequence Selectivity: A Stopped-Flow Kinetics Study of DNA/RNA Hybridization by Duplex- and Triplex-Forming Oligonucleotides[†]

Shaohui Wang,[‡] Alan E. Friedman,[§] and Eric T. Kool*[‡]

Department of Chemistry, University of Rochester, Rochester, New York 14627, and Johnson & Johnson Clinical Diagnostics, Rochester, New York 14650

ABSTRACT: Stopped-flow UV kinetics and thermal denaturation experiments are used to examine the origins of high sequence selectivity and binding affinity of circular triplex-forming oligonucleotides with single-stranded DNA/RNA targets. These 34-nt probes are hybridized to a series of 12-nt target sequences which are fully complementary or which contain a single mismatch. Also studied for comparison are standard 12-nt Watson-Crick DNA or RNA complements. Several novel findings are described: (1) Circular triplex-forming oligomers bind targets with very high thermodynamic selectivity (up to 8—10 kcal/mol against a single-nucleotide mismatch), while linear strands show only 2—3 kcal/mol selectivity. (2) Rates for triplex formation by circular ligands are much greater than other reported triplex formation modes and are nearly the same as for Watson—Crick duplex formation. (3) DNA—DNA and RNA—RNA hybridization rates are similar for both duplex and triplex formation. (4) For both modes of binding, hybridization rates do not vary when a mismatch is introduced into the target, and, therefore, binding selectivity is reflected in large variations in dissociation, rather than association rates. Finally, (5) binding selectivity of circular ligands becomes significantly greater as pH is lowered; results indicate that the high sequence selectivity of the circular DNA ligand is due in large part to the special stability of the protonated C+G-C triad relative to unprotonated mismatched triads. The results are useful in the understanding of properties of nucleic acid complexes in general and give insight into optimum design for synthetic DNA-binding ligands.

The fidelity of base pairing interactions in nucleic acids plays a crucial role in the functioning of biological systems. Several studies have addressed sequence selectivities of complexation in RNA and DNA duplexes (Aboul-ela et al., 1985; Werntges et al., 1986; Freier et al., 1986), and recently studies have examined selectivity of triplex formation, involving third-strand hybridization with duplexes, as well (Roberts & Crothers, 1991; Rougée et al., 1992; Best & Dervan, 1995). Recent studies involving the design of nonnatural nucleic acid-binding structures have brought increasing attention to the question of sequence selectivity. The proposed use of synthetic or otherwise engineered nucleic acid analogs as selective probes of sequence (Strobel et al., 1991) or as agents for modification of gene expression (Uhlmann & Peyman, 1990) gives the issue practical importance. For example, the use of synthetic backbone-modified DNA analogs (Beaucage & Iyer, 1993) to bind natural sequences and inhibit gene expression requires high pairing fidelity so that closely related sequences are not inhibited. The possible use of catalyic RNAs to cleave disease-related RNA sequences (Uhlenbeck, 1987) also brings up similar issues of sequence-selectivity.

Some novel strategies for increasing sequence selectivity have been reported recently. For example, by sacrificing some binding affinity, it is possible to design internal secondary structure into an oligonucleotide which competes with binding to incorrect sequences more effectively than it competes with binding to a complementary sequence (Roberts & Crothers, 1991). In many applications, particularly when direct inhibition of polymerase or ribosomal processing is desired, a high affinity of binding is useful, however. High affinity and high binding selectivity are not necessarily mutually exclusive properties: by engineering added rigidity into a ligand, both properties can be simultaneously enhanced. With that idea in mind, we synthesized triplex-forming circular oligonucleotides as ligands for single strands of DNA (Prakash & Kool, 1991, 1992) and RNA (Wang & Kool, 1994), and this design has led to compounds with very high binding affinity and among the highest DNA sequence selectivities yet characterized (Kool, 1991).

Because of such benefits in affinity and selectivity, the general strategy of binding single-stranded nucleic acids by triple helix formation has received rapidly increasing attention in several laboratories worldwide (Giovannangeli, 1991; D'Souza & Kool, 1992, 1994; Rumney & Kool, 1992; Salunkhe et al., 1992; Rubin et al., 1993; Giovannangeli et al., 1993; Gryaznov & Lloyd, 1993; Hudson & Damha, 1993; Kandimal & Agrawal, 1994; Wang & Kool, 1994a; Noll et al., 1994; Trapane & Ts'o, 1994; Reynolds et al., 1994). Study of the kinetic and thermodynamic properties of such triplex-forming ligands is needed to understand the origins of these benefits. Such understanding may be useful in the

  * To whom correspondence should be addressed.
  [‡] University of Rochester.
  [§] Johnson & Johnson Clinical Diagnostics.

design of further improvements in nucleic acid-binding molecules.

While a number of studies exist on the kinetics of binding for DNA or RNA duplexes [reviewed in Turner et al. (1990)], few studies have explored the effect of mismatches on binding kinetics. For DNA duplexes one study used temperature-jump and stopped-flow techniques and found that duplex association rates did not vary with the presence of a mismatch (Tibanyenda et al., 1984). Similar studies have not been performed, to our knowledge, with RNA duplexes. As for triple helical structures, there exist a few studies measuring the rate of third-strand binding to preformed DNA duplexes (Maher et al., 1990; Rougée et al., 1992; Shindoe et al., 1993; Yang et al., 1994); however, there are no previous reports on the rate of triplex formation with a single-stranded DNA target. In addition, while early polymer studies have given some information on triplex formation rates (Blake & Fresco, 1966; Blake et al., 1967, 1968; Porschke & Eigen, 1971), there are no other reports in existence on the kinetics of any triple-helical RNA complex in short, sequence-defined oligonucleotides.

For these reasons we undertook the investigation of kinetic and thermodynamic details of the binding of circular DNA and RNA oligonucleotide probes to a series of complementary and mismatched target oligonucleotides. These circular probes form complexes with purine-rich target strands by binding the target between opposing sides of the pyrimidine-rich ligand, forming a bimolecular triple helix. A preliminary report described increased thermodynamic selectivities of a circular DNA relative to a linear oligodeoxynucleotide (Kool, 1991). In an effort to understand the origins of this high selectivity, we now examine the kinetics of association using stopped-flow methods. New thermal denaturation data for both DNA and RNA complexes are obtained and compared to results obtained with standard Watson−Crick complementary oligomers. The effects on selectivity of varied pH, mismatch position, and the specific base triad involved are examined as well.

EXPERIMENTAL PROCEDURES

Oligonucleotide Synthesis. DNA oligonucleotides were synthesized on a Pharmacia LKB automated synthesizer or an Applied Biosystems (ABI) 392 synthesizer using standard β-cyanoethylphosphoramidite chemistry (Beaucage & Caruthers, 1981). RNA oligonucleotides were prepared using *tert*-butyl(dimethylsilyl)-protected phosphoramidites (Applied Biosystems) and following published oligoribonucleotide synthesis procedures (Ogilvie et al., 1988; Scaringe et al., 1990). The precursor to the circular RNA oligomer was synthesized with a single dC nucleoside at the 3′ terminus to ensure 3′−5′ isomeric purity at the linkage. 5′-Phosphorylation was carried out with a commercially available phosphoramidite reagent (Horn & Urdea, 1986) (Glen Research). Tetrabutylammonium fluoride in THF (Aldrich) was dried over molecular sieves prior to use in the desilylation step for compounds containing RNA residues (Hogrefe et al., 1993). Oligomers were purified by preparative 20% denaturing polyacrylamide gel electrophoresis and quantitated by absorbance at 260 nm. Molar extinction coefficients for the oligonucleotides were calculated by the nearest neighbor method (Borer, 1985).

The cyclization of the 5′-phosphorylated precursors to give circular ligands **1** and **3** was carried out as previously

described (Wang & Kool, 1994). The circular products were isolated by preparative denaturing gel electrophoresis. Circularity was confirmed by nicking with S1 nuclease or by partial alkaline hydrolysis; circles give a single initial degradation product which migrates with the linear precursor.

Melting Studies. Solutions for the thermal denaturation studies contained a one-to-one ratio of linear or circular probe oligomer and 12-nucleotide complementary purine target oligomer (1.5 μM each). Also present were 100 mM NaCl and 10 mM $MgCl_2$. Solutions were buffered with 10 mM Na-PIPES [1,4-piperazinebis(ethanesulfonate), Sigma] at pH 7.0 or 5.5. The buffer pH is that of a 1.4× stock solution at 25 °C containing the buffer and salts. After the solutions were prepared they were heated to 90 °C and allowed to cool slowly to room temperature prior to the melting experiments.

The melting studies were carried out in teflon-stoppered 1 cm path length quartz cells under nitrogen atmosphere on a Varian Cary 1 UV−vis spectophotometer equipped with thermoprogrammer. Absorbance (260 nm) was monitored while temperature was raised at a rate of 0.5 °C/min; a slower heating rate with this apparatus does not affect the results. Several cases were melted using both heating and cooling cycles, and the two curves very nearly superimposed, indicating very little hysteresis. In all cases the complexes displayed sharp, apparently two-state transitions, with all-or-none melting from bound complex to free oligomers. Melting temperatures (T_m) were determined from a nonlinear least squares fit of the melting data (see below) and were taken from the first derivative of absorbance with respect to $1/T$. Uncertainty in T_m is estimated at ±0.5 °C based on repetitions of experiments. Melting runs for RNA complexes repeated after an initial melting experiment showed little change in T_m or curve shape, indicating that there is little if any degradation of the RNA under these conditions.

Free energy values were derived by nonlinear least-squares fitting of the denaturation data, using a two-state model for melting with linear sloping baselines (Petersheim & Turner, 1983). van't Hoff thermodynamic parameters derived from $1/T_m$ vs $\ln(C_T/4)$ were independently measured for circle **1** with its 12-nt complement, with three mismatched targets, and at three pH values; for all six cases, close agreement was seen (within 1−15%) with the results from curve-fitting, indicating that the two-state approximation is a reasonable one for this sequence. Uncertainty in individual free energy measurements is estimated at $\pm10\%$.

Stopped-Flow Kinetics. Kinetics experiments were performed generally under pseudo-first-order conditions on a Sequential DX17 MV stopped-flow apparatus (Applied Photophysics Leatherhead, U.K.). The sample handling unit was fitted with two drive syringes that are mounted inside a thermostated bath compartment. Each DNA or RNA target strand was prepared as a solution at 5 μM concentration in a buffer containing 100 mM NaCl, 10 mM $MgCl_2$, and 10 mM Na•PIPES at the pH indicated. Each DNA or RNA ligand was prepared as a solution at 0.5μM concentration in the same salt and buffer. Both solutions were injected simultaneously at 25 °C, and the formation of the complex was monitored by the change in UV absorption at 260 nm. The optical-detection cell had a 10 mm path length. First-order curve fitting and rate constants used a Marquardt algorithm (Marquardt, 1963) based on the routine Curfit (Bevington, 1969). Absorption spectra at indicated time

A

(1) deoxy- (circular)
(2) 5'-d-CTTTTCTTTCTT

(3) ribo- (circular)
(4) 5'-r-CUUUUCUUUCUU

B

bimolecular duplex formation

5'-d-AAGAAAGAAAAG
+
5'-d-CTTTTCTTTCTT
$\xrightarrow{k_{assoc}}$ $\xleftarrow{k_{diss}}$
5'-d-AAGAAAGAAAAG
TTCTTTCTTTTC-d-5'
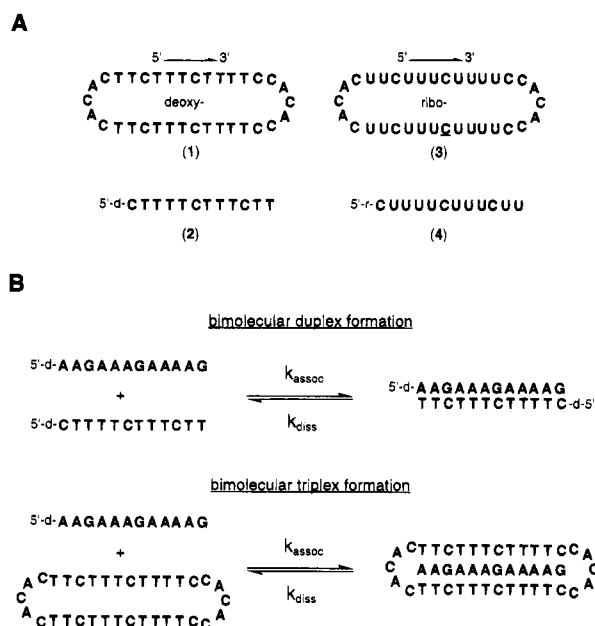
bimolecular triplex formation

FIGURE 1: (A) Sequences of the DNA and RNA ligands used in this study to bind to DNA and RNA purine-rich targets. Note that the underlined nucleotide in the RNA circular ligand is a 2'-deoxyribonucleotide. (B) Formation of duplex and triplex from linear and circular oligonucleotide ligands with purine-rich target strands (DNA ligand and target are shown as an example). In the triple-helical complex, the lower domain of the circle binds to the target in the antiparallel Watson—Crick mode, while the upper domain binds in the parallel Hoogsteen mode.

points were calculated through software provided by Applied Photophysics. This consisted of slicing the appropriate time points across a series of kinetic traces (at different wavelengths) and then splining the points of a specific time group (Detty et al., 1994). For each complex, the rate constant is reported as the average of values from ten injections. Precision in the averaged rate constant is $\pm 7\%$ or less. Concentration and volumetric errors may also affect the accuracy of the reported rate constant; we estimate these to be at most $\pm 10-15\%$.

RESULTS

Thermodynamic Selectivity Studies: DNA—DNA Complexes. Circular oligodeoxynucleotide **1** (see Figure 1) has been previously shown to form a bimolecular triple-helical complex with DNA complements having the sequence dAAGAAAGAAAAG (Wang & Kool, 1994). Because of the three C-G-C triads formed, this complex is pH dependent and is approximately half protonated at pH 7.0 (D'Souza & Kool, 1994). To measure equilibrium association constants (K_{assoc}), we carried out thermal denaturation experiments monitored at 260 nm. Stopped-flow mixing experiments were used to measure bimolecular association rates (with rate constants k_{assoc}); rates of dissociation (k_{diss}) were then derived from K_{assoc} and k_{assoc} assuming two-state binding for the bimolecular complexes.

The thermal denaturation studies were carried out using circular and linear DNA oligomers **1** and **2** (Figure 1) as probes for hybridization to a series of complementary and singly-mismatched 12-mer target sequences (Table 1). The mismatches are located at three different positions and are paired with T or with C in the probe strand. The experiments were carried out in the presence of 100 mM NaCl and 10

Table 1: Melting Temperatures (T_m) and Free Energies ($-\Delta G°_{25}$) for Complexes of Linear and Circular Oligodeoxyribonucleotides with Complementary and Mismatched DNA Target Strands at pH 7.0, Mismatched Bases Underlined

target sequences	T_m[a,b] (°C)	ΔT_m[c] (°C)	$-\Delta G°_{25}$[a,b] (kcal)	$\Delta\Delta G°_{25}$[c] (kcal)
probe strand: 3'- d(TT CT TT CT TTT C)				
5'- d(AAGAAAGAAAAG)	38.8	-	11.9	-
5'- d(AAGAAGGAAAAG)	31.6	7.1	10.0	1.9
5'- d(AAGAACGAAAAG)	27.1	11.7	9.0	2.9
5'- d(AAGAATGAAAAG)	27.5	11.3	8.9	3.0
5'- d(GAGAAAGAAAAG)	38.6	0.2	12.5	-0.6
5'- d(CAGAAAGAAAAG)	37.4	1.4	11.9	0.0
5'- d(TAGAAAGAAAAG)	38.2	0.6	11.5	0.4
probe strand: (circular CTTCTTTCTTTTCC)				
5'- d(AAGAAAGAAAAG)	54.5	-	18.1	-
5'- d(AAGAAGGAAAAG)	37.5	17.0	11.5	6.6
5'- d(AAGAACGAAAAG)	34.8	19.7	10.6	7.5
5'- d(AAGAATGAAAAG)	35.9	18.6	11.1	7.0
5'- d(AAGAAAAAAAAG)	35.1	19.4	11.0	7.1
5'- d(AAGAAACAAAAG)	34.3	20.2	10.8	7.3
5'- d(AAGAAATAAAAG)	33.0	21.5	10.6	7.5
5'- d(GAGAAAGAAAAG)	49.5	5.0	17.0	1.1
5'- d(CAGAAAGAAAAG)	48.0	6.5	16.4	1.7
5'- d(TAGAAAGAAAAG)	48.2	6.3	16.0	2.1

[a] Conditions: 3.0 μM total strand concentration, 100 mM NaCl, 10 mM MgCl$_2$, 10 mM Na-PIPES buffer. [b] Error limits for individual measurements are estimated at ± 0.5 °C in T_m and $\pm 10\%$ in free energy. Data shown are the averages from three measurements. [c] ΔT_m and $\Delta\Delta G°_{25}$ values are obtained by subtracting the values of the mismatched complexes from those of the fully complementary complexes.

mM MgCl$_2$, using an equimolar mixture of probe and target at a total strand concentration of 3.0 μM.

Examination of T_m values and free energies of association for the two fully complementary complexes of **1** and **2** at neutral pH confirm earlier findings that such circular compounds bind considerably more strongly than do linear Watson—Crick oligonucleotides to a complementary purine-rich strand (Prakash & Kool, 1991, 1992). Circular compound **1** binds its complement with a free energy ($\Delta G°_{25}$) of -18.1 kcal/mol, compared with -11.9 kcal/mol for the linear oligomer **2**. This corresponds to a difference of more than four orders of magnitude in association constant under these conditions.

Comparison of T_m and free energy values of complementary and mismatched sequences gives a measurement of sequence selectivity. Results for the standard duplex show (Table 1) that at neutral pH the Watson—Crick probe **2** shows a small amount of sensitivity to a T-X mismatch at a central position. The mismatches at this position result in a drop in T_m of $7-12$ °C and a loss in free energy of binding of $2-3$ kcal/mol, values that are consistent with literature data for duplex mismatches (Aboul-ela et al., 1985; Werntges et al., 1986; Kool, 1991). We have previously studied C-X mismatches in a closely related sequence (Kool, 1991); that study measured ΔT_m and $\Delta\Delta G°$ values of $17-22$ °C and

5.2−5.8 kcal/mol, respectively, which are somewhat higher than for T-X mismatches.

When circular probe oligomer **1** is hybridized to the same series of targets as was the linear probe **2**, however, the results reveal considerably higher thermodynamic selectivity for the cyclic compound. Values of ΔT_m are found to be 17−20 °C for a single T-X-T mismatch, and $\Delta\Delta G°$'s associated with the mismatches are 6.6−7.5 kcal/mol at 25 °C. Mismatches for the circular probe were also examined in a C-X-C pairing position, with varied base X in the target strand. Results from this second series at pH 7.0 are quite similar to those with the T-X-T mismatch: T_m values drop by 19−22 °C on substitution by mismatched bases, and free energies drop by 7.1−7.5 kcal/mol. Thus, there seems to be very little difference in selectivity between T-X-T and C-X-C triads at neutral pH.

Effects of Mismatch Position on Selectivity. The disruption of binding by mismatches is known to be greater near the center of a duplex than for mismatches at the end (Freier et al., 1986; Petruska et al., 1988). We compared the end-position sensitivity of linear and circular ligands for the same mismatch series; this position is paired opposite T residues in the two probes. Table 1 shows the effects of mismatches at the extreme 5′ end position of the 12-nt target sequence.

Both sets of data for the linear and circular probes show that selectivity at the end position is considerably lower than at a central position. For example, the linear probe **2** gives a drop in T_m of 1.4 °C or less for all three of the possible mismatches. The free energy of association also changes very little, falling within 0.6 kcal/mol of zero. However, the circular probe **1** shows significant binding selectivity even at this extreme end position. The mismatches cause a drop in T_m of 5.0−6.5 °C and a reduction in free energy of binding of 1−2 kcal/mol. This free energy difference corresponds to a selectivity in association constant of 6−35-fold against a single mismatch at the end position of the 12-nt sequence. Thus, while the selectivity at this position is considerably lower than at a central position, the circle retains significant sensitivity against end-positioned mismatches, while the linear probe does not.

Effects of pH on Binding Selectivity. The binding affinities of triple-helical DNA complexes involving C-G-C triads are well known to be sensitive to pH (Lipsett, 1964); however, the effects of pH on binding sequence selectivity have not, to our knowledge, been studied previously. In a closely related circular DNA complex, the cytosines in the Hoogsteen strand have an average pK_a of approximately 7.0−7.5 (D'Souza & Kool, 1994), and so, at neutral pH, the three cytosines in the present complex are expected to be approximately half protonated. To test the effect of changing protonation state on selectivity, we examined the binding of circular compound **1** to the complementary and mismatched oligomers at varied pH. Table 2 lists T_m values and free energies for the resulting complexes.

Results show that, for the fully complementary triplex, the free energy of complexation becomes 14.9 kcal/mol more favorable on lowering pH from 8.5 to 5.5; this is associated with an increase in T_m of 20 °C. This increasing complex strength corresponds to a change of approximately 3.5 kcal per pK unit. Since the protonation state of the complex increases from approximately zero to three protons over this range, the binding affinity increase also corresponds to an increase of ~3.5 kcal/mol of affinity per proton or positive

Table 2: Effects of pH on Melting Temperatures and Free Energies for Triple-Helical Complexes of Circular DNA (**1**) with DNA Target Strands of Varied Sequences, Mismatched Bases Underlined

target sequences	T_m [a,b] (°C)	ΔT_m [c] (°C)	$-\Delta G°_{25}$ [a,b] (kcal)	$\Delta\Delta G°_{25}$ [c] (kcal)
pH=5.5				
5′- d(AAGAAAGAAAAG)	68.8	-	25.5	-
5′- d(AAGAAA<u>A</u>AAAAG)	49.9	18.9	17.3	8.2
5′- d(AAGAAA<u>C</u>AAAAG)	49.6	19.2	17.0	8.5
5′- d(AAGAAA<u>T</u>AAAAG)	45.0	23.8	15.1	10.4
pH=7.0				
5′- d(AAGAAAGAAAAG)	54.5	-	18.1	-
5′- d(AAGAAA<u>A</u>AAAAG)	35.1	19.4	11.0	7.1
5′- d(AAGAAA<u>C</u>AAAAG)	34.3	20.2	10.8	7.3
5′- d(AAGAAA<u>T</u>AAAAG)	33.0	21.5	10.6	7.5
pH=8.5				
5′- d(AAGAAAGAAAAG)	49.0	-	14.9	-
5′- d(AAGAAA<u>A</u>AAAAG)	32.5	16.5	10.8	4.1
5′- d(AAGAAA<u>C</u>AAAAG)	30.4	18.6	10.2	4.7
5′- d(AAGAAA<u>T</u>AAAAG)	31.1	17.5	10.4	4.5

[a] Conditions: 3.0 μM total strand concentration, 100 mM NaCl, 10 mM MgCl$_2$, 10 mM Na-PIPES buffer. [b] Error limits for individual measurements are estimated at ±0.5 °C in T_m and ±10% in free energy. Data shown are the averages from three measurements. [c] ΔT_m and $\Delta\Delta G°_{25}$ values are obtained by subtracting the values of the mismatched complexes from those of the fully complementary complexes.
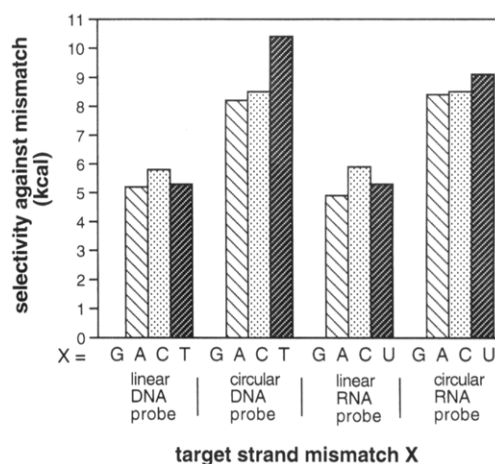
FIGURE 2: Histograms of maximum selectivities against specific single C-X (or C-X-C) mismatches for duplex-forming and triplex-forming DNA or RNA probes binding the sequence 5′-AA-GAAAXAAAAG [X = A, C, G, T(U)]. Data for duplexes were taken at pH 7.0, and for triplexes, pH 5.5.

charge. The binding of a given mismatched target strand is also pH dependent, as expected since two other C-G-C triads are present in the complex. For example, the C-C-C mismatched complex increases in strength by 6.8 kcal/mol on decreasing the pH from 8.5 to 5.5; this corresponds to ~2.3 kcal per pK unit. This is a significantly lower dependence than seen for the fully complementary complex.

When the free energies (or T_m values) of the mismatched complexes are subtracted from those of the complementary complex at a given pH value, one obtains selectivity ($\Delta\Delta G°$ or ΔT_m) values for the circular oligomer **1** at that pH. Figure 2 shows histograms of selectivity for linear and circular DNA probes; Figure 3 displays the general effects of pH on selectivities of circles **1** and **3**. It is clear (Figure 2) that the
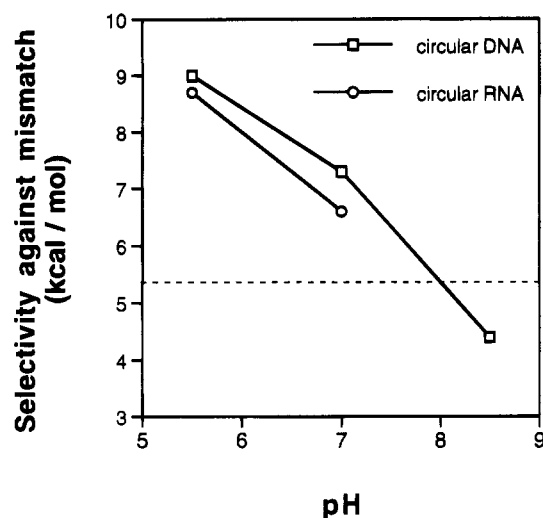
FIGURE 3: pH dependence of sequence selectivity for circular ligands **1** and **3**. Plotted are the average free energies of selectivity against mismatches (C-X-C) at varied pH. Horizontal dotted line indicates the corresponding selectivity of linear duplex-forming DNA or RNA oligonucleotides **2** and **4** (C-X mismatch).

circular ligands can have a strong selectivity advantages over linear Watson–Crick probes.

Interestingly, the pH studies show that circular ligand **1** shows much higher sequence selectivity at pH 5.5 than it does at pH 8.5. The average selectivity against one C-X-C mismatch is 4.4 kcal/mol at the high pH value but increases to 9.0 kcal/mol at the lower pH (Figure 3). This large selectivity corresponds to a difference in association constant of seven orders of magnitude at pH 5.5. We have previously measured the mismatch stabilities for C-X pairs in a closely related duplex, and the average selectivity in that case was 5.4 kcal/mol (see dotted line in Figure 3). It seems that the circular ligand has superior selectivity relative to a duplex-forming probe at pH 5.5 and 7.0, but not at pH 8.5. In general, it is clear that magnitude of the circular ligand's sequence selectivity is strongly dependent on pH.

Thermodynamic Selectivity Studies: RNA–RNA Complexes. To determine whether the differences in structure and conformation of RNA complexes relative to DNA complexes lead to differences in binding kinetics, we measured equilibrium association constants and association rate constants for circular (**3**) and linear (**4**) RNA probes having the same sequence as the DNAs **1** and **2** (Figure 1). The T_m and free energy data for neutral pH are presented in Table 3; for the linear and circular RNAs, we examined binding to the correct complement and to sets of mismatches paired opposite U or C residues at positions near the center of the complexes. Conditions for the thermal denaturations were the same as for the DNA experiments.

At neutral pH the circular RNA ligand binds the fully complementary RNA target with stability higher than that of the duplex by a small margin, as previously reported (Wang & Kool, 1994). The advantage for the circular compound is 4.9 °C in T_m and 0.9 kcal/mol in free energy (25 °C). In terms of selectivity, the linear RNA probe (**4**) binding RNA gives results not markedly different those seen for the linear DNA probe with a DNA target. The substitution of single mismatched bases at this position results in a drop of 3.8–14.2 °C in T_m and 1.4–4.2 kcal/mol in binding affinity at 25 °C. The results do show that the U-G pair is

Table 3: Melting Temperatures and Free Energies for Complexes of Linear and Circular Oligoribonucleotides with Complementary and Mismatched RNA Target Strands at pH 7.0

target sequences	T_m [a,b] (°C)	ΔT_m [c] (°C)	$-\Delta G°_{25}$ [a,b] (kcal)	$\Delta\Delta G°_{25}$ [c] (kcal)
probe strand: 3'- r(UUCUUUCUUUUC)				
5'- r(AAGAAAGAAAAG)	46.5	-	14.5	-
5'- r(AAGAAGGAAAAG)	42.7	3.8	13.1	1.4
5'- r(AAGAACGAAAAG)	32.3	14.2	10.3	4.2
5'- r(AAGAAUGAAAAG)	34.2	12.3	10.9	3.6
5'- r(AAGAAAAAAAAG)	22.6	23.9	7.9	6.6
5'- r(AAGAAACAAAAG)	22.0	24.5	7.6	6.9
5'- r(AAGAAAUAAAAG)	24.0	22.5	8.1	6.4
probe strand: $_A$CUUCUUUCUUUUCC$_A$ / ^{A}CUUCUUUCUUUUCC^A (circular)				
5'- r(AAGAAAGAAAAG)	51.2	-	15.4	-
5'- r(AAGAAGGAAAAG)	44.1	7.1	13.9	1.5
5'- r(AAGAACGAAAAG)	37.5	13.7	11.1	4.3
5'- r(AAGAAUGAAAAG)	36.7	14.5	11.8	3.6
5'- r(AAGAAAAAAAAG)	32.0	19.2	10.5	4.9
5'- r(AAGAAACAAAAG)	29.9	21.3	9.5	5.9
5'- r(AAGAAAUAAAAG)	31.2	20.0	10.1	5.3

[a] Conditions: 3.0 μM total strand concentration, 100 mM NaCl, 10 mM MgCl₂, 10 mM Na-PIPES buffer. [b] Error limits for individual measurements are estimated at ±0.5 °C in T_m and ±10% in free energy. Data shown are the averages from three measurements. [c] ΔT_m and $\Delta\Delta G°_{25}$ values are obtained by subtracting the values of the mismatched complexes from those of the fully complementary complexes.

significantly more stable than other mismatches, as has been previously noted (Aboul-ela et al., 1985). The U-G mismatch in this context is somewhat less destabilizing in a relative sense than is a T-G mismatch in DNA: the U-G mismatch has a ΔT_m of 3.8 °C and a $\Delta\Delta G°$ of 1.4 kcal, while the T-G mismatch in DNA has a ΔT_m of 7.1 °C and a $\Delta\Delta G°$ of 1.9 kcal/mol (see Tables 1 and 3). As for the DNA duplex, C-X (where X = A, T, C, G) mismatches are energetically more costly, with $\Delta\Delta G°$ values of 6.4–6.9 kcal/mol.

Effects of pH on Binding Selectivity. The results show that the circular RNA ligand shows no added selectivity advantage over a linear RNA probe at neutral pH, although it does have a small advantage in binding affinity. However, as with the circular DNA complex, at a lower pH of 5.5 the circular RNA binds its RNA complement more strongly and more selectively (Table 4). The effects of changing pH on matched and mismatched RNA complexes were examined in experiments analogous to those carried out for the DNA complexes. Results show that the selectivity is again seen to be dependent on pH, with increased ΔT_m and $\Delta\Delta G°$ values observed at pH 5.5 relative to those obtained at pH 7.0. We did not examine behavior at higher pH values because the system shows essentially no added selectivity and very weak third-strand interaction at neutral pH, and raising the pH further would not be expected to increase such an interaction.

The ΔT_m and $\Delta\Delta G°$ values at two pH values and for two mismatch positions are presented in Table 4, and the effects of pH on selectivity are plotted in Figure 3. The data show that while selectivity of the circular RNA **3** is not high at

Table 4: Effects of pH on Melting Temperatures and Free Energies for Complexes of Circular RNA Oligoribonucleotide (3) with Complementary and Mismatched RNA Target Strands

target sequences	T_m [a,b] (°C)	ΔT_m [c] (°C)	$-\Delta G°_{25}$ [a,b] (kcal)	$\Delta\Delta G°_{25}$ [c] (kcal)
pH = 7.0				
5'-r(AAGAAAGAAAAG)	51.2	-	15.4	-
5'-r(AAGAA**G**GAAAAG)	44.1	7.1	13.9	1.5
5'-r(AAGAA**C**GAAAAG)	37.5	13.7	11.1	4.3
5'-r(AAGAA**U**GAAAAG)	36.7	14.5	11.8	3.6
pH = 5.5				
5'-r(AAGAAAGAAAAG)	62.9	-	21.1	-
5'-r(AAGAA**G**GAAAAG)	51.1	11.8	14.8	6.3
5'-r(AAGAA**C**GAAAAG)	43.8	19.1	13.2	7.9
5'-r(AAGAA**U**GAAAAG)	44.1	18.8	13.2	7.9
pH = 7.0				
5'-r(AAGAAAGAAAAG)	51.2	-	15.4	-
5'-r(AAGAAA**A**AAAAG)	32.0	19.2	13.9	4.9
5'-r(AAGAAA**C**AAAAG)	29.9	21.3	11.1	5.9
5'-r(AAGAAA**U**AAAAG)	31.2	20.0	11.8	5.3
pH = 5.5				
5'-r(AAGAAAGAAAAG)	62.9	-	21.1	-
5'-r(AAGAAA**A**AAAAG)	42.9	20.0	12.7	8.4
5'-r(AAGAAA**C**AAAAG)	42.2	20.7	12.6	8.5
5'-r(AAGAAA**U**AAAAG)	39.4	23.5	12.0	9.1

[a] Conditions: 3.0 μM total strand concentration, 100 mM NaCl, 10 mM MgCl$_2$, 10 mM Na-PIPES buffer. [b] Error limits for individual measurements are estimated at ± 0.5 °C in T_m and $\pm 10\%$ in free energy. Data shown are the averages from three measurements. [c] ΔT_m and $\Delta\Delta G°_{25}$ values are obtained by subtracting the values of the mismatched complexes from those of the fully complementary complexes.

Table 5: Association Rates as a Function of Varying Concentration for Binding of a Circular Triplex—Forming Oligomer with Its Complement at pH 7.0

circular ligand concentration	target strand concentration	association rate [a] (M•s⁻¹)
0.5 μM	1.0 μM	0.47 x 10⁻⁶
0.5 μM	0.5 μM	0.28 x 10⁻⁶
0.5 μM	0.25 μM	0.12 x 10⁻⁶
1.0 μM	0.5 μM	0.44 x 10⁻⁶
0.5 μM	0.5 μM	0.28 x 10⁻⁶
0.25 μM	0.5 μM	0.14 x 10⁻⁶

ligand:
$$_A^{C\ T\ T\ C\ T\ T\ T\ C\ T\ T\ T\ T\ C\ C}A$$
$$ C\quad\quad\quad\quad\quad\quad\quad\quad\quad C$$
$$_A^{C\ T\ T\ C\ T\ T\ T\ C\ T\ T\ T\ T\ C\ C}A$$
target: dAAGAAAGAAAAG

[a] Obtained from stopped-flow experiments in 100 mM NaCl, 10 mM MgCl$_2$, and 10 mM Na-PIPES buffer (25 °C).

neutral pH, it increases markedly at pH 5.5. Examination of mismatches opposite C (in a C-X-C triad) show an average selectivity of 8.7 kcal against a mismatch at this lower pH. These values are similar to those seen for the circular DNA **1**. Thus, increasing protonation of the C-G-C triad in the RNA triplex favors selectivity, as it does for DNA triplexes; Figure 3 points out the similarity of the two.

The results show that selectivity is also pH dependent at a U-X-U triad adjacent to a C-G-C triad (Table 4). At pH 7.0 the average selectivity against a mismatch is 3.3 kcal/ mol, but at pH 5.5 this increases to 7.3 kcal/mol. Since U-X-U triads are not expected to be dependent on pH, this effect probably arises from the adjacent C-G-C triad; this possibility is discussed below. Finally, as was seen for the DNA triplexes, the RNA mismatches show lower changes in selectivity as a function of pH than do the fully complementary triplexes.

Kinetics of Binding: DNA—DNA Complexes. The selectivity data for probes **1** and **2** are thermodynamic parameters which can be expressed as differential association constants (K_{assoc}) for complementary and mismatched target sequences (Table 5). For example, the linear probe **2** prefers to bind to its complement by approximately one to two orders of magnitude in association constant relative to a singly mismatched target. The circular probe, by comparison, prefers its complement by about five to six orders of magnitude in K_a. Under the two-state binding model the equilibrium constant, K_{assoc}, is the quotient of the binding rate constant (k_{assoc}) over the dissociation rate constant (k_{diss}), and the differences in K_{assoc} seen in the selectivity experi-

ments could be reflected in differences in k_{assoc}, in k_{diss}, or a combination of both.

We measured the association rates of the bimolecular double and triple-helical complexes using stopped-flow UV methods at 25 °C, following the drop in absorbance at 260 nm as helix formation proceeds. Some experiments were carried out under second-order conditions to establish kinetic order in the separate DNA strands (see below). The majority of the kinetics experiments were carried out under pseudo-first-order conditions, with a 10-fold excess of target strand over ligand. Figure 4 shows typical decay curves for triplex and duplex hybridizations. The apparent first-order rate constants were derived by a curve-fitting algorithm (Marquardt, 1963; Bevington, 1969), and each mixing experiment was carried out 10 times and the results averaged for increased precision. Second-order rate constants were then derived from the apparent first-order rate constants and the known concentrations of ligand and target. The results for both DNA and RNA complexes are presented in Tables 5—7.

Association Rates. To understand better the high selectivities and binding affinities seen for circular DNA ligand **1**, we measured association rates for matched and mismatched triplexes involving that ligand and compared them to duplexes involving linear DNA oligomer **2**. Table 5 shows data obtained under second-order conditions with varied concentrations of **1** and its target. Table 6 lists equilibrium binding constants and association rate constants measured under pseudo-first-order conditions for duplexes and triplexes at 25 °C and neutral pH and additionally for the circle complexes at pH 5.5 and 8.5.

Variation of the concentrations of circle **1** and its complement were used to establish kinetic order of the two reactants (Table 5). Each oligomer was varied from 0.25 to 1.0 μM while the other was held constant; results show that each 2-fold change in concentration led to a corresponding 2-fold change in rate. This held true for both reactants. Thus, the overall binding kinetics are first order with respect both to circle **1** and its complement, and the overall kinetics are second order.

The majority of the kinetics runs were carried out under pseudo-first-order conditions to simplify curve fitting and

A

B

FIGURE 4: Typical stopped-flow kinetics runs in this study, showing primary data with the best-fit single-exponential curve superimposed. Data are taken at pH 7.0, 25 °C. (A) DNA circle **1** binding the complement 5'-dAAGAAAGAAAAG. (B) Linear DNA probe 5'-CTTTTCTTTCTT (**2**) binding the complement 5'-dAAGAAA-GAAAAG.

increase the accuracy of the results. The kinetic data were generally well-behaved for both the linear and circular cases and were fit well by a single-exponential, pseudo-first-order decay curve (Figure 4). Results show (Table 6) that for the linear DNA probe **1** with its complement, association rate constants agree well with literature values for DNA duplex formation involving short synthetic sequences. The average second-order rate constant in our study for this case was 4.4 $\times$ 10^6 M^{-1} s^{-1}. This compares favorably with literature values of 0.3−12 $\times$ 10^6 M^{-1} s^{-1} measured in other studies (Nelson & Tinoco, 1982; Williams et al., 1989; Turner et al., 1990).

Kinetics measurements involving the three mismatched duplexes (Table 6) show that association rates are nearly the same as those for the complementary case. The rate constants vary only from 3.3 to 5.8 $\times$ 10^6 M^{-1} s^{-1} for the three mismatches, or very close to the rate constant for the fully complementary duplex. A previous study of the effects of mismatches on duplex DNA association kinetics using temperature-jump methods found that mismatches had no effect on the rate of association (Tibanyenda et al., 1984); the present results are in agreement with that finding.

Interestingly, results of kinetics experiments using the circular DNA probe show that it forms complexes at nearly the same rate as the duplexes. The rate constant for circular **1** with its complement at pH 7.0 (25 °C) is found to be 5.7 $\times$ 10^6 M^{-1} s^{-1} (Table 6). In addition, as for duplex, the rates of mismatched complex formation are essentially the same as those for the fully complementary triplex, ranging from 2.4 to 7.1 $\times$ 10^6 M^{-1} s^{-1}. Thus, the data show that neither duplex nor triplex formation for these sequences is

Table 6: Kinetic Data for Complexes of Linear and Circular Oligodeoxyribonucleotides with Complementary and Mismatched DNA Target Sequences at Varied pH

target sequences	K_a[a] (M^{-1})	k_{assoc}[b] (M^{-1}s^{-1})	k_{diss}[c] (s^{-1})	$t_{1/2}$[c]
probe strand: 3'-d(T T C T T T C T T T T C)				
pH=7.0				
5'- d(AAGAAAGAAAAG)	5.4e^8	4.4e^6	8.1e^{-3}	85 sec
5'- d(AAGAA**G**GAAAAG)	2.2e^7	5.3e^6	2.4e^{-1}	2.9 sec
5'- d(AAGAA**C**GAAAAG)	4.0e^6	5.8e^6	1.4	0.5 sec
5'- d(AAGAA**T**GAAAAG)	3.4e^6	3.3e^6	9.7e^{-1}	0.7 sec
probe strand: ^{A}C$^{CTTCTTT CTTTTCC}$$_A$ $_C$^{ACTTCTTTCTTTTCC}^{A}				
pH=7.0				
5'- d(AAGAAAGAAAAG)	1.9e^{13}	5.7e^6	3.0e^{-7}	27 days
5'- d(AAGAA**G**GAAAAG)	2.7e^8	7.1e^6	2.6e^{-2}	27 sec
5'- d(AAGAA**C**GAAAAG)	6.0e^7	3.6e^6	6.0e^{-2}	12 sec
5'- d(AAGAA**T**GAAAAG)	1.4e^8	2.4e^6	1.7e^{-2}	41 sec
pH=5.5				
5'- d(AAGAAAGAAAAG)	5.3e^{18}	3.7e^6	7.0e^{-13}	3.1e^4 yr
5'- d(AAGAAA**A**AAAAG)	4.8e^{12}	3.5e^6	7.3e^{-7}	11 days
5'- d(AAGAAA**C**AAAAG)	2.8e^{12}	3.0e^6	1.1e^{-6}	7.5 days
5'- d(AAGAAA**T**AAAAG)	1.1e^{11}	2.0e^6	1.8e^{-5}	11 hr
pH=8.5				
5'- d(AAGAAAGAAAAG)	8.3e^{10}	4.7e^6	5.7e^{-5}	3.4 hr
5'- d(AAGAAA**A**AAAAG)	8.3e^7	2.4e^6	2.9e^{-2}	24 sec
5'- d(AAGAAA**C**AAAAG)	3.3e^7	1.5e^6	4.5e^{-2}	15 sec
5'- d(AAGAAA**T**AAAAG)	4.5e^7	2.3e^6	5.1e^{-2}	14 sec

[a] Derived from the free energies in Tables 1 and 2. [b] Obtained from stopped-flow experiments in 100 mM NaCl, 10 mM MgCl$_2$, 10 mM Na-PIPES buffer (25 °C). Data are the averages of 10 measurements. Standard deviations of the averages are at most 7%. [c] Calculated from K_a and k_{assoc}.

changed by the presence of single mismatched bases; in addition, there is no apparent difference in the rate of bimolecular duplex or triplex formation.

To establish that the drop in absorbance being monitored for the circular ligand corresponds to true three-stranded, cooperative complex formation, and not merely rapid duplex formation followed by a slower third-strand binding, we followed a hybridization reaction for as long as 50 half-lives, and there was no additional drop in absorbance seen. This confirms that complete hybridization has occurred. A separate experiment carried out by simple mixing in a UV−vis spectrometer (data not shown) confirms that circle binding is much more rapid than third-strand triplex formation: binding of circle **1** to 5'-dAAGAAAGAAAAG was complete in less than 15 s (at 0.75 μM concentration each strand), while binding of the Hoogsteen-complementary 5'-dCTTTTCTTTCTT to a preformed complementary duplex could be readily observed, taking ca. 120 s to drop to a steady-state absorbance. A third confirmation of rapid triplex formation by the circular ligand is found in optical melting experiments: heating and cooling curves show little if any hysteresis, unlike third-strand binding, which shows a lag in binding on the cooling part of the cycle (Rougée et al., 1992). Finally, absorption spectra of the binding reaction taken at successive time intervals show clear isosbestic points, as expected for a two-state association.

Dissociation Rates. Since we have obtained values both for equilibrium binding constants and for association rate constants, this allows the calculation of dissociation rates for circular and linear probes **1** and **2** when bound to fully complementary or singly mismatched target sequences. Table 6 shows the k_{diss} values calculated for all the DNA cases, along with $t_{1/2}$ data (the half-life for dissociation at 25 °C) derived from the k_{diss} values.

Comparison of calculated dissociation rate constants for the linear probe **2** and circular probe **1** shows that there are large differences between the double- and triple-helical complexes. For example, at pH 7.0 and 25 °C the linear probe dissociates with a rate constant of 8.1×10^{-3} s^{-1}, while that for the circle complex is 3.0×10^{-7} s^{-1}, or more than four orders of magnitude slower. Comparison of dissociation rates for mismatched complexes with these two probes shows a much smaller difference. For example, the mismatched duplexes have an average k_{diss} of 0.9 s^{-1}, whereas the mismatched circle complexes have an average k_{diss} of 0.03 s^{-1}, or 30-fold slower. Thus, the largest differences between the duplex and circle triplex are found in the very slow dissociation of the circle relative to the linear probe from the complementary strand.

Further examination of the data for the Watson−Crick duplexes shows (Table 6) that the dissociation rates for the duplexes are significantly higher for mismatched complexes than for the fully complementary case. This is expected since the binding constants vary significantly, while the association rates do not. For example, the T-T mismatch dissociates at a rate 120-fold higher than the complementary duplex. The half-life ($t_{1/2}$) for dissociation is 85 s for the complementary duplex and averages 1.4 s for the three mismatched cases.
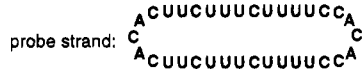
By contrast, the calculated dissociation rate constants for the circular oligodeoxynucleotide at neutral pH are much more sensitive to mismatches. The T-T-T mismatched complex, for example, dissociates at a rate which is nearly five orders of magnitude faster than for the complementary T-A-T case. The half-life for dissociation is calculated to be 27 days for the complementary complex, while the mismatched complexes have half-lives averaging 27 s.

Effects of pH on Association and Dissociation Rates for a Circular DNA. The association and dissociation rates for the C-X-C series with circular compound **1** were then examined as a function of pH. Two extremes of pH (5.5 and 8.5) were studied (Table 6). Overall examination of the rate constants for association show only small variations as a result of changing pH, both for complementary and mismatched complexes. All of the rate constants are approximately the same within experimental error and fall in the range $2-8 \times 10^6$ M^{-1} s^{-1}.

In contrast to this, the calculated dissociation rates for the circular probe vary to a large degree with changing pH. For the fully complementary complex at pH 5.5, the dissociation rate constant is 7.0×10^{-13} s^{-1}; on increasing pH to 8.5, k_{diss} increases greatly to 5.7×10^{-5} s^{-1}, for a difference of nearly 8 orders of magnitude at the two pH extremes. Half-lives for the complex range from 3.4 h at pH 8.5 (25 °C) to a calculated 31 000 years at pH 5.5.

The dissociation rates for the singly mismatched complexes of circle **1** are also pH dependent, but not to as large a degree as the complementary complex. For example, the C-T-C mismatched complex has a k_{diss} of 1.8×10^{-5} s^{-1} at pH 5.5, and it increases to 5.1×10^{-2} s^{-1} at pH 8.5, for a

Table 7: Kinetic Data for Complexes of Linear and Circular Oligoribonucleotides with Complementary and Mismatched RNA Target Sequences at pH 7.0

target sequences	$K_a{}^a$ (M^{-1})	$k_{assoc}{}^b$ ($M^{-1}s^{-1}$)	$k_{diss}{}^c$ (s^{-1})	$t_{1/2}{}^c$
probe strand: 3'- r(UUCUUUCUUUUC)				
5'- r(AAGAAAGAAAAG)	$4.3e^{10}$	$6.9e^6$	$1.6e^{-4}$	1.2 hr
5'- r(AAGAAGGAAAAG)	$4.1e^9$	$10.8e^6$	$2.6e^{-3}$	4.4 min
5'- r(AAGAACGAAAAG)	$3.6e^7$	$6.2e^6$	$1.7e^{-1}$	4.1 sec
5'- r(AAGAAUGAAAAG)	$9.9e^7$	$5.2e^6$	$5.2e^{-2}$	13 sec
probe strand: ^{A}CUUCUUUCUUUUC^C_A C----C ^{A}CUUCUUUCUUUUC^A				
5'- r(AAGAAAGAAAAG)	$2.0e^{11}$	$8.8e^6$	$4.4e^{-5}$	4.4 hr
5'- r(AAGAAGGAAAAG)	$1.6e^{10}$	$10.1e^6$	$6.3e^{-4}$	18 min
5'- r(AAGAACGAAAAG)	$1.4e^8$	$6.5e^6$	$4.6e^{-2}$	15 sec
5'- r(AAGAAUGAAAAG)	$4.5e^8$	$6.2e^6$	$1.4e^{-2}$	49 sec

^{a} Derived from the free energies in Table 3. ^{b} Obtained from stopped-flow experiments in 100 mM NaCl, 10 mM MgCl₂, 10 mM Na-PIPES buffer (25 °C). Data are the averages of 10 measurements. Standard deviations of the averages are at most 7%. ^{c} Calculated from K_a and k_{assoc}.

total range of 2800-fold (Table 6). The other mismatched complexes behave similarly, with changes in k_{diss} of $\sim 10^3-10^4$-fold at the two pH extremes. Thus, the fully complementary triplex shows much greater pH sensitivity (in terms of dissociation rates) than do the mismatched complexes.

Kinetics of Binding: RNA−RNA Complexes. Eight complementary or mismatched probe−target combinations were examined for the kinetics of binding, using the same methods as for the DNA complexes described above. In general, results show that, as for the DNA case, the association rates show little dependence on whether the probes are linear or circular, or whether the targets are fully complementary or mismatched. The data from these experiments are presented in Table 7.

Association Rates. The stopped-flow experiments with the linear 12-mer probe strand **4** show that association rate constants are not significantly dependent on whether the target is fully complementary or singly mismatched. The range of rate constants is $5.2-10.8 \times 10^6$ M^{-1} s^{-1} (Table 7). For the circular probe, rate constants are essentially the same: the overall range is $6.2-10.1 \times 10^6$ M^{-1} s^{-1}. As for the linear probe, the circular RNA hybridization is apparently not affected, within our experimental error, by the presence of single mismatches in the target strand.

The average of all eight rate constants for the RNA-RNA hybridizations is $7.6 (\pm 1.9) \times 10^6$ M^{-1} s^{-1}. Interestingly, the corresponding average for the eight analogous DNA−DNA complexes is a lower $4.7 (\pm 1.5) \times 10^6$ M^{-1} s^{-1}. Thus, it would appear that the RNA−RNA complexes may be formed slightly more rapidly than are the DNA complexes, although any difference is clearly small. Tinoco previously found for a different duplex sequence that DNA−DNA hybridization was slightly faster than RNA−RNA hybridization (Aboul-ela et al., 1985).

Dissociation Rates. The data show that while the association rates for the RNA complexes are not affected by probe structure or by mismatches, the calculated dissociation rates are affected to a large degree. This is again consistent with

effects seen for the DNA complexes. As before, the dissociation rate constants (k_{diss}) and half-lives ($t_{1/2}$) were mathematically derived from the experimentally measured free energies and the measured association rates. The data are presented in Table 7.

Results for the RNA−RNA duplexes show that the dissociation rates are increased by the presence of single mismatches. This increase ranges from 16-fold for a U-G mismatch to 1000-fold for a U-C mismatch. The half-life for the complementary complex (25 °C) is 1.2 h, and those for the mismatched targets are 4.1 s to 4.4 min.

Comparison of dissociation rates for the linear and circular probes at pH 7.0 shows that there are only small differences between the two, consistent with the finding that the overall binding properties are not very different at neutral pH. For both complementary and mismatched targets the circular ligand dissociates approximately 4-fold more slowly. For example, the fully complementary complex has a half-life of 4.4 h at pH 7.0 (25 °C). The circle itself shows kinetic selectivity against mismatches which are virtually identical to those for the linear probe; the increase in dissociation rates range from 14-fold to 1000-fold, depending on the specific mismatch involved. We did not measure pH effects on RNA association rates, but since the circular RNA binds much more strongly at pH 5.5 (Table 4) than at neutral pH, it is probable that rates of dissociation are considerably less at the lower pH value.

DISCUSSION

Unusual Association and Dissociation Rates for Triplex Formation on a Single-Stranded Target. The rate constants found here for triplex formation with a single-stranded target are considerably greater than those reported for third-strand binding to a preformed duplex DNA (Maher et al., 1990; Rougée et al., 1992; Shindoe et al., 1993; Yang et al., 1994). Previous studies have used several different methods for measurement of rate constants. Dervan and co-workers used an endonuclease inhibition assay and measured a rate constant of 2.0×10^3 M^{-1} s^{-1} for binding of a 21-mer DNA to a longer duplex (Maher et al., 1990). Hélène and co-workers, using a hysteresis assay, found rate constants of as high as 2.0×10^4 M^{-1} s^{-1} at high magnesium concentrations (Rougée et al., 1992). Shindoe et al. (1993) reported a rate constant of 2.1×10^3 M^{-1} s^{-1} using filter-binding methods, and Yang et al. (1994) found a rate constant of 2.7×10^3 M^{-1} s^{-1} using fluorescence methods. While there is some variation in these values, ranging from $\sim 10^3$ to 10^4 M^{-1} s^{-1}, there is clear consensus that the third-strand binding is much slower (by 100−10 000-fold) than rates for duplex formation. Thus, our measured rate for triplex formation on a single-stranded target is much more rapid (by $\sim 2-4$ orders of magnitude) than third-strand triplex formation on a duplex target.

The fact that bimolecular triplex formation has essentially the same rate as duplex formation suggests that the rate-limiting steps for the two complexes may be similar. Duplex DNA formation has a low activation barrier which is associated with rate-limiting nucleation of a small number of base pairs (Wetmur & Davidson, 1968; Porschke & Eigen, 1971); this is then followed by rapid hybridization of the remaining base pairs. In such a mechanism there is no reason to expect that a single mismatch would affect the rate, and

that is what is observed. In the case of triplex formation on a single-stranded target, it is possible that the same mechanism operates: rate-limiting nucleation occurs either in the Watson−Crick or Hoogsteen domains; the remaining hybridization is then rapid to complete formation of the full triplex. The other mode of triplex formation, third strand binding to a preformed duplex, is significantly slower than this because some structural reorganization is likely required prior to hybridization (Rougée et al., 1992). This reorganization may involve a conformational change (such as a B to A form transition) or removal of coordinated water molecules or metal ions in the major groove. In the present case, such a prior reorganization is not required, since the target is single-stranded and thus lacks the strong secondary structure such as is present in duplex DNA. Such rapid hybridization rates are desirable in practical biological applications; rapid binding (coupled with rapid dissociation from mismatched sites) allows a probe to find binding sites in a large genome more efficiently and selectively.

The binding of complementary sequences by such triplex-forming ligands is very high-affinity in nature. High-affinity binding can be associated with very rapid complexation, very slow dissociation, or both. In the present case, since association rates do not vary for duplex or triplex formation, this implies that the tight binding is coupled with lower dissociation rates. Indeed, the dissociation rates calculated here for the complexes of the circular triplex-forming DNA are extremely slow. For example, the circular ligand has a calculated half-life of nearly a month at neutral pH, while a duplex formed with a standard Watson−Crick-forming probe has a half-life under the same conditions of less than 2 min. High-affinity binding can be useful when hybridization is required at very low probe concentrations or under stringent conditions, such as in conditions of low salt or high temperature. In addition, tight binding, and slow dissociation in particular, can lead to potentially useful biological properties such as the blockade-like ability to inhibit polymerase progression along a DNA or RNA strand or progression of the ribosome along an RNA strand.

Kinetic Origins of High Sequence Selectivity. The sequence selectivity of the triplex-forming circular ligands is extremely high relative to standard linear probes. Again, because association rates for the two cases are the same, and because they do not vary with mismatches, this selectivity difference arises from differential dissociation rates. A circular triplex-forming ligand dissociates five to six orders of magnitude more rapidly from a mismatched target than it does from a complementary target at pH 7.0. By contrast, a linear probe dissociates only $\sim 10-100$-fold more rapidly in the presence of a mismatch. Large selectivities such as those seen here can be useful in providing a larger window of specific binding. This means that conditions for stringent binding require less careful control in diagnostic hybridizations. When biological activity is desired, there is a wider range of conditions which will give specific activity without giving some nonspecific activity due to partially mismatched complexes.

Cytosine Protonation Increases Sequence Selectivity. The data provided here give insight into the physical and structural reasons for the high selectivity of triplex-forming ligands. It is clear that the sequence selectivity of the circular ligand is pH dependent and that this is related to the protonation of the C-G-C triad. The total selectivity is as

large as 8−10 kcal/mol, which is 3−4 kcal greater than the selectivity of a single linear probe. Comparing selectivities at pH 5.5 relative to pH 8.5, we find that the magnitude of the pH-dependent contribution to selectivity is approximately 4.5 kcal/mol (Figure 3); thus, this protonation effect is perhaps the major reason why the circular ligand is more selective than the linear one.

It is thus apparent that, when binding a single-stranded nucleic acid, the majority of the added selectivity of a triplex-forming oligonucleotide (relative to a Watson−Crick probe) arises from the special stability of the protonated C+G-C triad. This favorable protonation is likely to be largely an electrostatic effect (Völker & Klump, 1994): the added positive charge partially ameliorates backbone negative charge repulsions.

How does this cytosine protonation increase selectivity? It has been shown that cytosines in such a triplex are much more basic (by as much as 3 pK units) in the complex than when alone in solution (Callahan et al., 1991; D'Souza & Kool, 1994). This effect is likely due at least in part to the fact that the proton is shared between two bases in the triplex: the cytosine N-3 and guanine N-7. The resulting shift to an apparent pK_a of 7.0−7.5 enables such triplexes to be substantially protonated—and therefore stabilized—at pH values near neutral. However, when the cytosine is paired with a mismatch, the cytosine effectively becomes much less basic, and the possibility of protonation is lost near neutral pH. Consistent with this idea is the finding of lower pH dependence of C-X-C mismatched complexes relative to fully complementary ones.

Interestingly, we find that even a U-X-U triad, when adjacent to a C+G-C triad, shows pH dependence of its selectivity against mismatches. Such U-A-U or T-A-T triads are by themselves not dependent on pH changes over the range studied here (D'Souza & Kool, 1994). Thus, we hypothesize that a mismatch directly adjacent to a C+G-C triad may cause some local structural disruption which inhibits the C and G from approaching close enough for sharing of the proton. This leads to the testable prediction that the farther away a mismatch is to a C+G-C triad, the less energetically disrupting it will be. On the whole it is interesting to note that C+G-C triads not only display higher selectivities themselves but also appear to increase selectivity around them.

This pH dependence of selectivity leads to the general conclusion that all triple-helix-forming ligands, if they make use of protonated C+G-C interactions, will gain from this added sequence selectivity. Analogs of cytosine have been developed recently to avoid the need for protonation (Ono et al., 1991; Koh & Dervan, 1992; Krawczyk et al., 1992; Miller et al., 1992; Xiang et al., 1994); while this may be desirable from the standpoint of gaining binding affinity at neutral or higher pH, it now seems clear that a considerable amount of pairing selectivity is likely to be sacrificed. The present result also points out that, if one has a choice in altering hybridization conditions, such as in diagnostic applications, then triplex-forming probes will give a large benefit in sequence selectivity at low, as opposed to high, pH values.

In addition, there may be an intrinsic, non-pK_a-related advantage of selectivity for such triplex-forming ligands as well. This effect may be explained by the presence of two separate interactions between the ligand and the target

strand: such ligands form both Watson−Crick and Hoogseen hydrogen bonds (including twice the normal number of stacking interactions) with the target. When a mismatched base is present in the central target strand, it disrupts the helix roughly twice the amount that disruption occurs in standard duplex mismatches. This is therefore a mechanism for magnifying selectivity. In general, the more strongly cooperative a ligand−target interaction is, the more structurally disrupting will be a given mismatch. Increased cooperativity in designed ligands can be achieved by rigidifying the ligand (Cram, 1987), limiting entropic freedom which would otherwise be costly on complexation. Such triplex-forming ligands benefit entropically by the physical linking of two separate binding domains; circularizing such ligands (joining the binding domains on both ends) gives even greater preorganization and thus results in even higher affinity and sequence selectivity (Prakash & Kool, 1992).

Effects of Mismatch Position on Selectivity. Linear oligonucleotide probes are especially prone to accepting mismatched targets when the mismatch occurs near the end of the recognition sequence (Freier et al., 1986; Petruska et al., 1988). The reason that mismatches are less disrupting near the end of the helix is presumably because of the greater flexibility in the chain there. A mismatch at the end position still allows favorable stacking interactions and also gives the end nucleotides greater entropic freedom in the complex.

We have shown that it is possible to increase recognition selectivity even at the extreme end position of the target sequence by using a circular triplex-forming ligand. This added selectivity probably arises from nearby protonation effects (discussed above) and from the presence of the nucleotide loop which links the two binding domains. Such a linking group is likely to lessen the entropic freedom of the DNA chain at this end position. If this is the case, then cyclic ligands which are linked at both ends of the triplex will retain added sequence selectivity at both ends of the target, while singly-linked triplex-forming ligands will gain this benefit only at one end. In general, engineering greater rigidity in DNA-binding ligands can increase both selectivity and binding affinity simultaneously.

Conclusions. The current study reveals several previously unreported kinetic and thermodynamic findings for the binding of single-stranded nucleic acids by triplex formation. Among these findings are (1) triplex-forming circular oligonucleotides hybridize with a complementary strand with a rate constant of 2−4 × 10^6 M^{-1} s^{-1}, which is 3−4 orders of magnitude faster than the rates reported for triple helix formation between a single pyrimidine strand and a duplex, (2) the association rate for such bimolecular triplex formation is the same as that for standard duplex formation, and thus may involve a similar rate-limiting step, (3) bimolecular RNA duplexes and triplexes are formed with rate constants similar to those of DNA complexes, (4) triplex-forming circular oligomers can display extraordinarily long half-lives for dissociation relative to standard Watson−Crick duplex-forming probes, (5) the high sequence selectivity of such a circular ligand is associated with large differences in dissociation, rather than association, rates with matched and mismatched targets, and finally, (6) the origin of this high sequence selectivity is largely due to the formation of favorable C+G-C protonated triads; this argues against the use of nonprotonated cytosine analogs if high selectivity is desired.

REFERENCES

Aboul-ela, F., Koh, D., Tinoco, I., Jr., & Martin, F. H. (1985) *Nucleic Acids Res. 13*, 4811−4824.

Best, G. C., & Dervan, P. B. (1995) *J. Am. Chem. Soc. 117*, 1187−1193.

Beaucage, S. L., & Caruthers, M. H. (1981) *Tetrahedron Lett. 22*, 1859−1862.

Beaucage, S. L., & Iyer, R. P. (1993) *Tetrahedron 49*, 6123−6194.

Bevington, P. R. (1969) *Data Reduction and Error Analysis for the Physical Sciences*, McGraw-Hill, New York.

Blake, R. D., & Fresco, J. R. (1966) *J. Mol. Biol. 19*, 145−160.

Blake, R. D., Massoulie, J., & Fresco, J. R. (1967) *J. Mol. Biol. 30*, 291−308.

Blake, R. D., Klotz, L. C., & Fresco, J. R. (1968) *J. Am. Chem. Soc. 90*, 3556−3562.

Borer, P. N. (1985) in *Handbook of Biochemistry and Molecular Biology* (Fasman, G. D., Ed.) 3rd ed., Vol. I, p 589, CRC Press, Cleveland, OH.

Callahan, D. E., Trapane, T. L., Miller, P. S., Ts'o, P. O. P., & Kan, L.-S. (1991) *Biochemistry 30*, 1650.

Cram, D. J. (1987) *Chemtech 17*, 120−125.

Detty, M. R., Friedman, A. E., & McMillam, M. (1994) *Organometallics 13*, 3338.

D'Souza, D. J., & Kool, E. T. (1992) *J. Biomol. Struct. Dyn. 10*, 141−152.

D'Souza, D. J., & Kool, E. T. (1994) *Bioorg. Med. Chem. Lett. 4*, 965−970.

Escudé, C., François, J.-C., Sun, J., Ott, G., Sprinzl, M., Garestier, T., & Hélène, C. (1993) *Nucleic Acids Res. 21*, 5547−5553.

Freier, S. M., Kierzek, R., Jaeger, J. A., Sugimoto, N., Caruthers, M. H., Neilson, T., & Turner, D. H. (1986) *Proc. Natl. Acad. Sci. U.S.A. 83*, 9373−9377.

Giovannangeli, C., Montenay-Garestier, T., Rougée, M., Chassignol, M., Thuong, N. T., & Hélène, C. (1991) *J. Am. Chem. Soc. 113*, 7775−7776.

Giovannangeli, C., Thuong, N. T., & Hélène, C. (1993) *Proc. Natl. Acad. Sci. U.S.A. 90*, 10013−10017.

Gryaznov, S. M., & Lloyd, D. H. (1993) *Nucleic Acids Res. 21*, 5909−5915.

Han, H., & Dervan, P. B. (1993) *Proc. Natl. Acad. Sci. U.S.A. 90*, 3806−3810.

Hogrefe, R. I., McCaffrey, A. P., Borozdina, L. U., McCampbell, E. S., & Vaghefi, M. M. (1993) *Nucleic Acids Res. 21*, 4739−4741.

Horn, T., & Urdea, M. (1986) *Tetrahedron Lett. 27*, 4705−4708.

Hudson, R. H. E., & Damha, M. J. (1993) *Nucleic Acids Symp. Ser. 29*, 97−99.

Kandimal, E. R., & Agrawal, S. (1994) *Gene 149*, 115−121.

Koh, J. S., & Dervan, P. B. (1992) *J. Am. Chem. Soc. 114*, 1470−1478.

Kool, E. T. (1991) *J. Am. Chem. Soc. 113*, 6265−6266.

Krawczyk, S. H., Milligan, J. F., Wadwani, S., Moulds, C., Froehler, B. C., & Matteucci, M. D. (1992) *Proc. Natl. Acad. Sci. U.S.A. 89*, 3761−3764.

Lipsett, M. N. (1964) *J. Biol. Chem. 239*, 1256−1260.

Maher, L. J., III, Dervan, P. B., & Wold, B. (1990) *Biochemistry 29*, 8820−8826.

Marquardt, D. W. (1963) *J. Soc. Indust. Appl. Math. 11*, 431.

Miller, P. S., Bhan, P., Cushman, C. D., & Trapane, T. L. (1992) *Biochemistry 31*, 6788−6793.

Nelson, J. W., & Tinoco, I., Jr. (1982) *Biochemistry 21*, 5289−5295.

Noll, D. M., O'Rear, J. L., Cushman, C. D., & Miller, P. S. (1994) *Nucleosides Nucleotides 13*, 997−1005.

Ogilvie, K. K., Usman, N., Nicoghosian, K., & Cedergren, R. J. (1988) *Proc. Natl. Acad. Sci. U.S.A. 85*, 5764.

Ono, A., Ts'o, P. O. P., & Kan, L.-S. (1991) *J. Am. Chem. Soc. 113*, 4032−4033.

Petersheim, M., & Turner, D. H. (1983) *Biochemistry 22*, 256−263.

Petruska, J., Goodman, M. F., Boosalis, M. S., Sowers, L. C., Cheong, C., & Tinoco, I., Jr. (1988) *Proc. Natl. Acad. Sci. U.S.A. 85*, 6252.

Porschke, D., & Eigen, M. (1971) *J. Mol. Biol. 62*, 361−381.

Prakash, G., & Kool, E. T. (1991) *J. Chem. Soc., Chem. Commun.*, 1161−1162.

Prakash, G., & Kool, E. T. (1992) *J. Am. Chem. Soc. 114*, 3523−3528.

Prakash, G., & Kool, E. T. (1994) *J. Chem. Soc., Chem. Commun.*, 676.

Reynolds, M. A., Arnold, L. J., Almazan, M. T., Beck, T. A., Hogrefe, R. I., Metzler, M. D., Stoughton, S. R., Tseng, B. Y., Trapane, T. L., Ts'o, P. O. P., & Woolf, T. M. (1994) *Proc. Natl. Acad. Sci. U.S.A. 91*, 12433−12437.

Roberts, R. W., & Crothers, D. M. (1991) *Proc. Natl. Acad. Sci. U.S.A. 88*, 9397−9401.

Roberts, R. W., & Crothers, D. M. (1992) *Science 258*, 1463−1466.

Rougée, M., Faucon, B., Mergny, J. L., Barcelo, F., Giovannangeli, C., Montenay-Garestier, T., & Hélène, C. (1992) *Biochemistry 31*, 9269−9278.

Rubin, E., McKee, T. L., & Kool, E. T. (1993) *J. Am. Chem. Soc. 115*, 360−361.

Rumney, S., & Kool, E. T. (1992) *Angew. Chem. 104*, 1686−1689; (1992) *Angew. Chem. Int. Ed. Engl. 31*, 1617−1619.

Salunkhe, M., Wu, T., & Letsinger, R. L. (1992) *J. Am. Chem. Soc. 114*, 8768−8772.

Scaringe, S. A., Francklyn, C., & Usman, N. (1990) *Nucleic Acids Res. 18*, 5433−5441.

Shindoe, H., Torigoe, H., & Akinori, S., (1993) *Biochemistry 32*, 8963−8969.

Strobel, S. A., Doucette-Stamm, L. A., Riba, L., Housman, D. E., & Dervan, P. B. (1991) *Science 254*, 1639−1642.

Tibanyenda, S., De Bruin, S., Haasnoot, C. A. G., van der Marel, G. A., van Boom, J. H., & Hilbers, C. W. (1984) *Eur. J. Biochem. 139*, 19−27.

Trapane, T. L., & Ts'o, P. O. P. (1994) *J. Am. Chem. Soc. 116*, 10437−10449.

Turner, D. H., Sugimoto, N., & Freier, S. M. (1990) in *Nucleic Acids* (subvolume C) (Saenger, W., Ed.) pp 201−227, Springer-Verlag, Berlin.

Uhlenbeck, O. C. (1987) *Nature 321*, 596−600.

Uhlmann, E., & Peyman, A. (1990) *Chem. Rev. 90*, 543.

Wang, S., & Kool, E. T. (1994a) *Nucleic Acids Res. 22*, 2326−2333.

Wang, S., & Kool, E. T. (1994b) *J. Am. Chem. Soc. 116*, 8857−8858.

Wang, S., & Kool, E. T. (1995) *Biochemistry 34*, 4125−4132.

Werntges, H., Steger, G., Riesner, D., & Fritz, H.-J. (1986) *Nucleic Acids Res. 14*, 3773−3790.

Wetmur, J., & Davidson, N. (1968) *J. Mol. Biol. 31*, 349−370.

Williams, A. P., Longfellow, C. E., Freier, S. M., Kierzek, R., & Turner, D. H. (1989) *Biochemistry 28*, 4283−4291.

Xiang, G., Soussou, W., & McLaughlin, L. W. (1994) *J. Am. Chem. Soc. 116*, 11155−11156.

Yang, M., Ghosh, S. S., & Millar, D. P. (1994) *Biochemistry 33*, 15329−15337.